Journal of Natural Disaster Science, Volume 17, Number 1, 1995, pp. 13-27

STORM SURGE FLOODING IN CITIES IN THE OSAKA BAY AREA

Hajime NAKAGAWA
Associate Professor, Disaster Prevention Research Institute, Kyoto University
Kazuya INOUE
Professor, Disaster Prevention Research Institute, Kyoto University
Kazuhito SHIMAMOTO
Ministry of Construction
and
Tetsuhiko UETSUKA
Graduate Student, Department of Civil Engineering, Kyoto University

(Received 14 July, 1995 and in revised form 8 December, 1995)

ABSTRACT

A numerical simulation model for the simultaneous analysis of storm surges and their inundation of a protected low-lying area is presented. After the model was checked, the effectiveness of current measures taken against storm surges in Osaka Bay was estimated for a "designed typhoon". "The worst course" for a typhoon in the Osaka Bay area, the approximately 30 km western course of the Muroto Typhoon, was examined. Effects of the typhoon's speed on the extent of the area inundated also were investigated. When a typhoon takes the above course, the areas flooded increase with the increase in its speed. Zones at risk of storm surge flooding after a sea-level rise due to the green house effect also were predicted with this simulation model.

1. INTRODUCTION

Cities facing Osaka Bay have experienced a number of severe flood disasters due to storm surges. As the low-lying city of Osaka is on the course of most incoming typhoons and is at the innermost bend of the bay where high energy storm surges become concentrated, it is destined to suffer damage from typhoons. On September 21, 1934, the Muroto Typhoon struck Osaka. The maximum water level was 4.2 m above O.P. (O.P.: the mean sea level of Osaka Bay), and 3,036 persons were killed by the storm surges generated. On September 3, 1950, 534 persons were killed by Typhoon Jane (maximum water level, O.P.+3.7 m), and on September 16, 1961, 194 people were killed by the Dai-ni Muroto Typhoon (maximum water level, O.P.+4.12 m). The Ise Bay Typhoon of September 26, 1959, which did not strike Osaka directly, caused the deaths of more than 5,000 persons because of storm surges; the highest number of storm surge deaths recorded in Japan.

The current gross population of the cities facing Osaka Bay is about 10 million. Although various countermeasures against storm surges have been taken after disastrous typhoons, there is still high damage potential because of the concentrated population in these cities, the large areas of highly developed private and public properties, and the dense concentration of life-line systems. Moreover, as no major typhoons have struck Osaka for more than 30 years, it is not known whether the present countermeasures against storm surges will be effective. In addition, as the mean water level will have risen about 65 cm by the end of the 21st century due to the global greenhouse effect, the scale of storm surges experienced is expected to increase.

To prevent or mitigate storm-surge disasters, we must be able to predict the scale of the surges and

KEY WORDS: Storm surge, Flooding, Typhoon, Osaka Bay Area, Sea-level rise

take effective countermeasures such as the construction of coastal embankments and tide gates. It also is important to be able to predict the weak points of countermeasures already in use, the areas that will be inundated, the damage costs, and how such disasters can be prevented. Numerical simulations of storm surges and the process of inundation can provide much useful information.

We here present a numerical simulation model which simultaneously analyzes the occurrence of storm surges and the process by which low-lying cities facing Osaka Bay are inundated. The effectiveness of the existing structures taken as countermeasures against storm surges around the bay also is examined. The worst course of a typhoon in the Osaka Bay area is examined on the basis of areas flooded by storm surges. The influence of the typhoon's speed on the area flooded also is investigated. Moreover, zones at risk of flooding due to storm surges after a rise in sea level are predicted with this simulation model.

2. BASIC EQUATIONS

2.1 *Storm Surges and Flooding*

The basic equations used to calculate both the storm surges on and inundation process in a protected low-lying area are depth-averaged horizontal two-dimensional momentum and continuity equations (see **Fig. 1**):

$$\frac{\partial M}{\partial t}+\frac{\partial (uM)}{\partial x}+\frac{\partial (vM)}{\partial y}=fN-gh\frac{\partial (h+z_b)}{\partial x}-\frac{h\partial p}{\rho\partial x}+\frac{\tau_{sx}}{\rho}-\frac{\tau_{bx}}{\rho} \tag{1}$$

$$\frac{\partial N}{\partial t}+\frac{\partial (uN)}{\partial x}+\frac{\partial (vN)}{\partial y}=-fM-gh\frac{\partial (h+z_b)}{\partial y}-\frac{h\partial p}{\rho\partial y}+\frac{\tau_{sy}}{\rho}-\frac{\tau_{by}}{\rho} \tag{2}$$

$$\frac{\partial h}{\partial t}+\frac{\partial M}{\partial x}+\frac{\partial N}{\partial y}=0 \tag{3}$$

where M and N are the water discharge per unit width for x (eastward) and y (northward), i.e., $M=uh$ and $N=vh$ (hereafter called the "flux"), u and v being the respective depth-averaged velocity components of the x and y directions; h is the water depth; z_b the elevation of the bed; p the atmospheric pressure; ρ the density of the sea water; f the Coriolis parameter; g the gravitational force per unit mass; τ_{bx} and τ_{by} are the respective shear stresses on the bed in the x and y directions; and τ_{sx} and τ_{sy} the shear stresses at the water surface in the x and y directions. Shear stress at the water surface is evaluated as

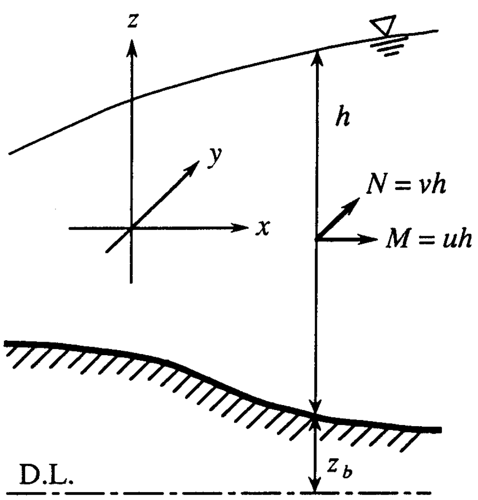

Fig. 1 Coordinate systems.

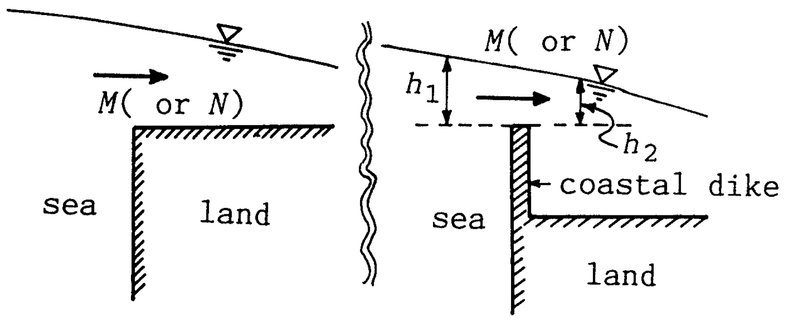

Fig. 2 Definition sketch of water overflow discharge.

$$\tau_{sx}=\rho_a f_s W_x \sqrt{W_x^2+W_y^2},\ \tau_{sy}=\rho_a f_s W_y \sqrt{W_x^2+W_y^2} \tag{4}$$

where ρ_a is the density of the air, f_s the resistance coefficient at the water surface, and W_x and W_y are the respective wind velocity components of the x and y directions at that surface. Bottom shear stress is assumed to take the relations

$$\tau_{bx}=\frac{\rho g n^2 u\sqrt{u^2+v^2}}{h^{1/3}}-k\tau_{sx}\ ,\ \tau_{by}=\frac{\rho g n^2 v\sqrt{u^2+v^2}}{h^{1/3}}-k\tau_{sy} \tag{5}$$

where n is Manning's roughness coefficient, and k a constant with the value 0.25 [1].

These equations are used to calculate storm surges and the flooding they produce. When there are no coastal embankments at the boundaries between the sea zones and land, flood discharge fluxes M and N can be calculated from these equations. When there are coastal embankments, the overflow discharge over the embankments can be evaluated; e.g., by the formulae [2]

$$\left.\begin{array}{ll} M\ (\text{or } N)=\mu h_1\sqrt{2gh_1} & (h_2/h_1 \leq 2/3) \\ M\ (\text{or } N)=\mu' h_2\sqrt{2g(h_1-h_2)} & (h_2/h_1 > 2/3) \end{array}\right\} \tag{6}$$

where μ and μ' are discharge coefficients with the respective values of 0.91 and 0.35; $h_1=H_r-H_o$; $h_2=H_f-H_o$; H_r is the water level on the seaward side; H_o the elevation of the coastal embankment crown, and H_f the water level on the landward side. In the calculations, h_1 and h_2 are defined at the cells adjacent to the coastal embankments. Overflow occurs when $h_1>0$ and $h_1>h_2$ (see **Fig. 2**) or $h_2>0$ and $h_2>h_1$. In the case that $h_1>0$ and $h_1>h_2$ the type of overflow is said to be "complete overflow" when $h_2/h_1>2/3$; whereas, there is "submerged overflow" when $h_2/h_1>2/3$ (see eq. (6)). M and N likewise can be evaluated for river dikes. It should be noted that the calculations for storm surges and the flooding produced are simultaneous, not separate.

2.2 *Typhoon Model*

First it is necessary to deal with the typhoon, the main external force and decider of the wind field in storm surge calculations. A number of typhoon models exist. We adopted Fujii and Mitsuta's model [3] because Yamashita obtained reasonable results with it [4]. In their model, an atmospheric pressure field is described by Schroemer's formula as

$$p=p_c+\Delta p\ \exp\left(-\frac{r_m}{r}\right) \tag{7}$$

where r is the distance from the center of the typhoon; p the pressure at the radial distance r; p_c the central pressure; Δp the difference between the peripheral and central pressures, and r_m the radius at the maximum wind speed.

The gradient wind speed, U_{gr} is obtained by solving the equation of motion

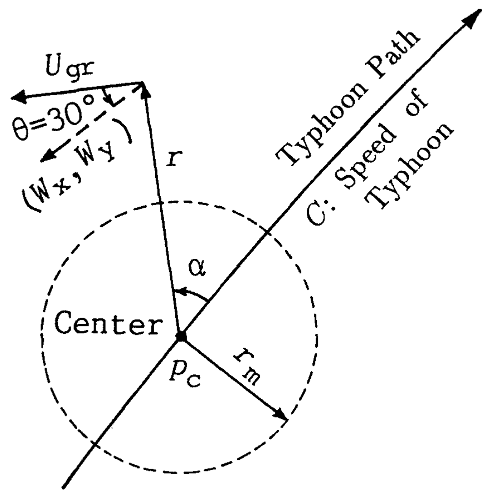

Fig. 3 Definition sketch of the typhoon model.

$$\frac{U_{gr}^2}{r_t}+fU_{gr}=\frac{1}{\rho_a}\frac{\partial p}{\partial r} \tag{8}$$

where r_t the radius of the curvature of the path line of the air cloud, is evaluated by Blaton's formula as

$$\frac{1}{r_t}=\frac{1}{r}\left(1+\frac{C}{U_{gr}}\sin\alpha\right) \tag{9}$$

where C is the typhoon's speed and α the direction angle of the radius vector measured counterclockwise from the direction of the movement of the typhoon (see **Fig. 3**). From Equations 7, 8, and 9, the gradient wind speed, U_{gr} is

$$U_{gr}=\frac{1}{2}\left\{-(C\sin\alpha+rf)+\sqrt{(C\sin\alpha+rf)^2+\frac{4\Delta p r_m}{\rho_a r}\exp\left(-\frac{r_m}{r}\right)}\right\} \tag{10}$$

The wind speed above the ground surface, U_s can be greater than the friction-free wind, U_{gr} a little inside and along the radius of the maximum typhonic wind speed. Mitsuta et al. confirmed this super-gradient wind effect in their analysis of recorded data for typhoons 7705 and 7709 that struck the Nansei Islands [5], [6]. Fujii and Mitsuta formulated this effect as

$$\frac{U_s}{U_{gr}}=G(\xi)=G(\infty)+\left\{G(\xi_p)-G(\infty)\right\}\left(\frac{\xi}{\xi_p}\right)^{m-1}\exp\left[\left(1-\frac{1}{m}\right)\left\{1-\left(\frac{\xi}{\xi_p}\right)^m\right\}\right] \tag{11}$$

where $\xi=r/r_m$. The parameters $m=2.5$, $\xi_p=0.5$, $G(\xi_p)=1.2$, and $G(\infty)=2/3$ are determined from these data. The function $G(\xi)$ increases with the increase in ξ, reaching the maximum value $G(\xi_p)$ at $\xi=\xi_p$. Thereafter it decreases with further increases in ξ, approaching $G(\infty)$ asymptotically at $\xi\rightarrow\infty$. The deflection angle of the surface wind to the isobars is assumed to be 30°. Consequently, the components of the wind speed at the position (x,y) in the storm surge calculations, W_x and W_y are

$$W_x=-\frac{(x-x_c)+\sqrt{3}(y-y_c)}{2r}U_s\ ,\quad W_y=\frac{\sqrt{3}(x-x_c)-(y-y_c)}{2r}U_s \tag{12}$$

where $(x_c,\ y_c)$ is the typhoon's position and $r^2=(x-x_c)^2+(y-y_c)^2$.

2.3 *Finite Difference Equations*

The system of equations is integrated numerically. The values to be calculated are the water depth, *h*, and the "flux", *M* and *N*. Fluxes *M*, *N* and the velocities *u*, *v* are defined in the middle of and normal

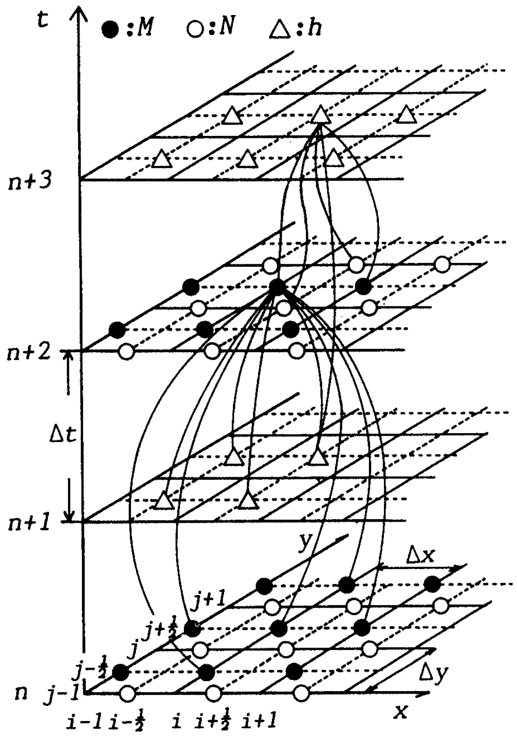

Fig. 4 Arrangement of variables and the order of calculation.

to each cell face. The water depth, h, is defined in the center of each cell. Therefore there are two staggered meshes associated with the respective "flux" (or velocity) components. The arrangement of the variables and calculation process are shown in **Fig. 4**. In this figure, (i, j) denotes the grid number, and n the time level. The derivatives approximated by finite differences lead to the following numerical forms of the equations [7]:

Finite difference equation for the continuity equation

$$\frac{h^{n+3}_{i+1/2,j+1/2}-h^{n+1}_{i+1/2,j+1/2}}{2\Delta t}+\frac{M^{n+2}_{i+1,j+1/2}-M^{n+2}_{i,j+1/2}}{\Delta x}+\frac{N^{n+2}_{i+1/2,j+1}-N^{n+2}_{i+1/2,j}}{\Delta y}=0 \tag{13}$$

Finite difference equation for the momentum equation of the x-component

$$\frac{M^{n+2}_{i,j+1/2}-M^{n}_{i,j+1/2}}{2\Delta t}$$

$$+\begin{cases} \dfrac{u^{n}_{i,j+1/2}M^{n}_{i,j+1/2}-u^{n}_{i-1,j+1/2}M^{n}_{i-1,j+1/2}}{\Delta x} & : u^{n}_{i,j+1/2}\geq 0,\ u^{n}_{i-1,j+1/2}>0 \\ \dfrac{u^{n}_{i,j+1/2}M^{n}_{i,j+1/2}-0}{\Delta x} & : u^{n}_{i,j+1/2}>0,\ u^{n}_{i-1,j+1/2}\leq 0 \\ \dfrac{u^{n}_{i+1,j+1/2}M^{n}_{i+1,j+1/2}-u^{n}_{i,j+1/2}M^{n}_{i,j+1/2}}{\Delta x} & : u^{n}_{i,j+1/2}\leq 0,\ u^{n}_{i+1,j+1/2}<0 \\ \dfrac{0-u^{n}_{i,j+1/2}M^{n}_{i,j+1/2}}{\Delta x} & : u^{n}_{i,j+1/2}<0,\ u^{n}_{i+1,j+1/2}\geq 0 \end{cases}$$

$$
+\begin{cases}
\dfrac{\tilde{v}^n_{i,j+1/2}M^n_{i,j+1/2}-\tilde{v}^n_{i,j-1/2}M^n_{i,j-1/2}}{\Delta y} & : \tilde{v}^n_{i,j+1/2}\geq 0,\ \tilde{v}^n_{i,j-1/2}>0 \\
\dfrac{\tilde{v}^n_{i,j+1/2}M^n_{i,j+1/2}-0}{\Delta y} & : \tilde{v}^n_{i,j+1/2}>0,\ \tilde{v}^n_{i,j-1/2}\leq 0 \\
\dfrac{\tilde{v}^n_{i,j+3/2}M^n_{i,j+3/2}-\tilde{v}^n_{i,j+1/2}M^n_{i,j+1/2}}{\Delta y} & : \tilde{v}^n_{i,j+1/2}\leq 0,\ \tilde{v}^n_{i,j+3/2}<0 \\
\dfrac{0-\tilde{v}^n_{i,j+1/2}M^n_{i,j+1/2}}{\Delta y} & : \tilde{v}^n_{i,j+1/2}<0,\ \tilde{v}^n_{i,j+3/2}\geq 0
\end{cases}
$$

$$
=-g\,\frac{h^{n+1}_{i-1/2,j+1/2}+h^{n+1}_{i+1/2,j+1/2}}{2}\cdot\frac{h^{n+1}_{i-1/2,j+1/2}+z_{bi+1/2,j+1/2}-h^{n+1}_{i-1/2,j+1/2}-z_{bi-1/2,j+1/2}}{\Delta x}
$$

$$
-\frac{h^{n+1}_{i+1/2,j+1/2}+h^{n+1}_{i-1/2,j+1/2}}{2\rho}\cdot\frac{p^{n+1}_{i+1/2,j+1/2}-p^{n+1}_{i-1/2,j+1/2}}{\Delta x}
$$

$$
-\frac{g\left(\dfrac{n_{i-1/2,j+1/2}+n_{i+1/2,j+1/2}}{2}\right)^2\dfrac{M^{n+2}_{i,j+1/2}+M^n_{i,j+1/2}}{h^{n+1}_{i-1/2,j+1/2}+h^{n+1}_{i+1/2,j+1/2}}\sqrt{(u^n_{i,j+1/2})^2+(\tilde{v}^n_{i,j+1/2})^2}}{\left(\dfrac{h^{n+1}_{i-1/2,j+1/2}+h^{n+1}_{i+1/2,j+1/2}}{2}\right)^{1/3}}
$$

$$
+\frac{\rho_a}{\rho}kf_sW_x\sqrt{W_x^2+\tilde{W}_y^2+f\tilde{v}^n_{i,j+1/2}}\,\frac{h^{n+1}_{i-1/2,j+1/2}+h^{n+1}_{i+1/2,j+1/2}}{2}+\frac{\rho_a}{\rho}\,f_sW_x\sqrt{W_x^2+\tilde{W}_y^2} \tag{14}
$$

Finite difference equation for the momentum equation of the y-component

$$
\frac{N^{n+2}_{i+1/2,j}-N^n_{i+1/2,j}}{2\Delta t}
$$

$$
+\begin{cases}
\dfrac{\tilde{u}^n_{i+1/2,j}N^n_{i+1/2,j}-\tilde{u}^n_{i+1/2,j-1}N^n_{i+1/2,j-1}}{\Delta x} & : \tilde{u}^n_{i+1/2,j}\geq 0,\ \tilde{u}^n_{i+1/2,j-1}>0 \\
\dfrac{\tilde{u}^n_{i+1/2,j}N^n_{i+1/2,j}-0}{\Delta x} & : \tilde{u}^n_{i+1/2,j}>0,\ \tilde{u}^n_{i+1/2,j-1}\leq 0 \\
\dfrac{\tilde{u}^n_{i+1/2,j+1}N^n_{i+1/2,j+1}-\tilde{u}^n_{i+1/2,j}N^n_{i+1/2,j}}{\Delta x} & : \tilde{u}^n_{i+1/2,j}\leq 0,\ \tilde{u}^n_{i+1/2,j+1}<0 \\
\dfrac{0-\tilde{u}^n_{i+1/2,j}N^n_{i+1/2,j}}{\Delta x} & : \tilde{u}^n_{i+1/2,j}<0,\ \tilde{u}^n_{i+1/2,j+1}\geq 0
\end{cases}
$$

$$
+\begin{cases}
\dfrac{v^n_{i+1/2,j}N^n_{i+1/2,j}-v^n_{i-1/2,j}N^n_{i-1/2,j}}{\Delta y} & : v^n_{i+1/2,j}\geq 0,\ v^n_{i-1/2,j}>0 \\
\dfrac{v^n_{i+1/2,j}N^n_{i+1/2,j}-0}{\Delta y} & : v^n_{i+1/2,j}>0,\ v^n_{i-1/2,j}\leq 0 \\
\dfrac{v^n_{i+3/2,j}N^n_{i+3/2,j}-v^n_{i+1/2,j}N^n_{i+1/2,j}}{\Delta y} & : v^n_{i+1/2,j}\leq 0,\ v^n_{i+3/2,j}<0 \\
\dfrac{0-v^n_{i+1/2,j}N^n_{i+1/2,j}}{\Delta y} & : v^n_{i+1/2,j}<0,\ v^n_{i+3/2,j}\geq 0
\end{cases}
$$

$$
=-g\,\frac{h^{n+1}_{i+1/2,j-1/2}+h^{n+1}_{i+1/2,j+1/2}}{2}\cdot\frac{h^{n+1}_{i+1/2,j+1/2}+z_{bi+1/2,j+1/2}-h^{n+1}_{i+1/2,j-1/2}-z_{bi+1/2,j-1/2}}{\Delta y}
$$

$$
-\frac{h^{n+1}_{i+1/2,j+1/2}+h^{n+1}_{i+1/2,j-1/2}}{2\rho}\cdot\frac{p^{n+1}_{i+1/2,j+1/2}-p^{n+1}_{i+1/2,j-1/2}}{\Delta y}
$$

$$-\frac{g\left(\dfrac{n_{i+1/2,j-1/2}+n_{i+1/2,j+1/2}}{2}\right)^2 \dfrac{N^{n+2}_{i+1/2,j}+N^{n}_{i+1/2,j}}{h^{n+1}_{i+1/2,j-1/2}+h^{n+1}_{i+1/2,j+1/2}}\sqrt{(\tilde{u}^{n}_{i+1/2,j})^2+(v^{n}_{i+1/2,j})^2}}{\left(\dfrac{h^{n+1}_{i+1/2,j-1/2}+h^{n+1}_{i+1/2,j+1/2}}{2}\right)^{1/3}}$$

$$+\frac{\rho_a}{\rho}kf_sW_y\sqrt{\tilde{W}^2_x+W^2_y}+f\tilde{u}^{n}_{i+1/2,j}\frac{h^{n+1}_{i+1/2,j-1/2}+h^{n+1}_{i+1/2,j+1/2}}{2}+\frac{\rho_a}{\rho}f_sW_y\sqrt{\tilde{W}^2_x+W^2_y} \tag{15}$$

where,

$$u^{n}_{i,j+1/2}=2M^{n}_{i,j+1/2}/(h^{n+1}_{i-1/2,j+1/2}+h^{n+1}_{i+1/2,j+1/2}),$$
$$v^{n}_{i+1/2,j}=2N^{n}_{i+1/2,j}/(h^{n+1}_{i+1/2,j-1/2}+h^{n+1}_{i+1/2,j+1/2}),$$
$$\tilde{u}^{n}_{i+1/2,j}=(u^{n}_{i,j-1/2}+u^{n}_{i+1,j-1/2}+u^{n}_{i,j+1/2}+u^{n}_{i+1,j+1/2})/4,$$
$$\tilde{v}^{n}_{i,j+1/2}=(v^{n}_{i-1/2,j}+v^{n}_{i-1/2,j+1}+v^{n}_{i+1/2,j}+v^{n}_{i+1/2,j+1})/4,$$
$$W_x=(W^{n+1}_{x;\,i-1/2,j+1/2}+W^{n+1}_{x;\,i+1/2,\,j+1/2})/2,$$
$$\tilde{W}_y=(W^{n+1}_{y;\,i-1/2,j+1/2}+W^{n+1}_{y;\,i+1/2,j+1/2})/2,$$
$$\tilde{W}_x=(W^{n+1}_{x;\,i+1/2,j-1/2}+W^{n+1}_{x;\,i+1/2,j+1/2})/2,$$
$$W_y=(W^{n+1}_{y;\,i+1/2,j-1/2}+W^{n+1}_{y;\,i+1/2,j+1/2})/2,$$

3. STORM SURGES IN OSAKA BAY

3.1 *Storm Surges Caused by the Dai-ni Muroto Typhoon*

On September 16, 1961, a severe typhoon, the Dai-ni Muroto Typhoon, struck Osaka. One hundred ninety-four people were killed, 4,972 injured, and 384,120 houses inundated. The typhoon's track is shown in **Fig. 5**, along with the tracks of the Muroto and Ise Bay typhoons. The track taken by the Muroto Typhoon is considered the most dangerous for cities situated on Osaka Bay. The Ise Bay Typhoon was the biggest and strongest typhoon ever to have struck Japan. It caused major disasters in the Kinki and Tokai districts.

We reproduced the storm surges caused by the Dai-ni Muroto Typhoon using the above typhoon model. There are two computational domains; a large scale domain with grid sizes Δx=1145 m for longitude and Δy=922.5 m for latitude, and a small scale domain with grid sizes Δx=286.25 m and Δy= 230.625 m (a quarter the length of the dimensions of the large scale domain). Only storm surges are calculated in the large scale domain in order to obtain the conditions at the open boundaries in the small scale domain. Results calculated for lines A-B and B-C in the large scale domain (**Fig. 6**) are stored in new data sets and used as boundary conditions in the small scale domain for the simultaneous calculation of storm surges and the flooding produced. In the large scale domain, astronomical tides at open boundaries (lines D-E and F-G in **Fig. 6**) are evaluated using the constituents of M_2, S_2, K_1, and O_1. The typhoon effect, the water surface being lifted by the drop in atmospheric pressure, and the wind set-up also considered at these boundaries are

$$\Delta h_p \text{ (cm unit)}=0.991(p_\infty-p) \text{ (hPa unit)} \tag{16}$$

$$\Delta h_w=\beta\Delta h_p \tag{17}$$

where Δh_p is the increment in the water level caused by the drop in pressure; p_∞ the peripheral pressure; Δh_w the increment in the water level caused by wind drift; and β the numerical constant [8].

Sea bed elevation data were obtained from bathymetric charts, and ground elevation data from topographical maps with the scale 1:2,500. The heights of the levee and coastal embankment crown are set along the sides of a cell. **Fig. 7** shows the ground elevation distribution in the small scale region. Ground heights along both sides of the Yodo River near its mouth are below 0 m mean sea level. As the population is very large and industries and businesses are concentrated in this area, the damage potential is extremely high.

The following values were used in the calculations: f=0.0000834 (1/sec), ρ_w=1030 (kg/m^3), ρ_a=1.293

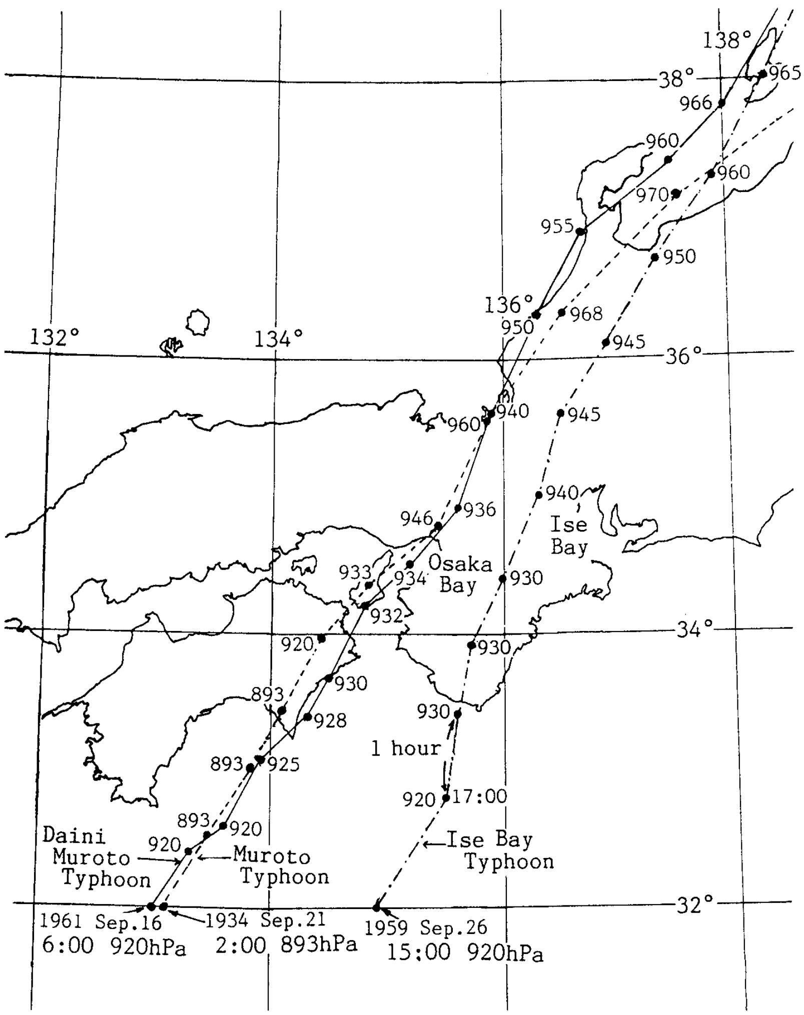

Fig. 5 Tracking paths of the Muroto, Ise Bay, and Dai-ni Muroto typhoons.

(kg/m^3), f_s=0.0026, r_m=60 (km), and β=1.0. For Manning's roughness coefficient, n=0.02 was used for the sea bed and n=0.067 for the land bed. The time step, Δt, was 10 seconds for the large scale domain and 2 seconds for the small one.

Fig. 8 shows a comparison of the calculated results for the small scale region and recorded water level data at Tannowa, Kobe, and Osaka North Port. In this figure, M.S.L. is the mean sea level for Osaka Bay. The results calculated for the forerunner parts are in fairly good agreement with recorded values at the three ports. The peak value of the calculated water level at Osaka North Port is about 3.4 m from the M.S.L., recorded as 2.8 m. For the resurgence part, the calculated water levels vary much more than the observed ones. The differences between the actual and calculated wind fields which result from the typhoon model probably are the cause of these discrepancies; but, there may be limitations to the application of the depth-integrated model for storm surges, as well.

3.2 *Existing Countermeasures against Storm Surges*

Cities located on Osaka Bay, including Osaka City, often have suffered from storm surges. Although countermeasures against storm surges were taken after Typhoon Jane in 1950, Osaka was again severely damaged by the Dai-ni Muroto Typhoon of 1961. One factor that has led to the increased seriousness of storm surge damage has been land-subsidence; therefore, soon after the Dai-ni Muroto Typhoon, a three-

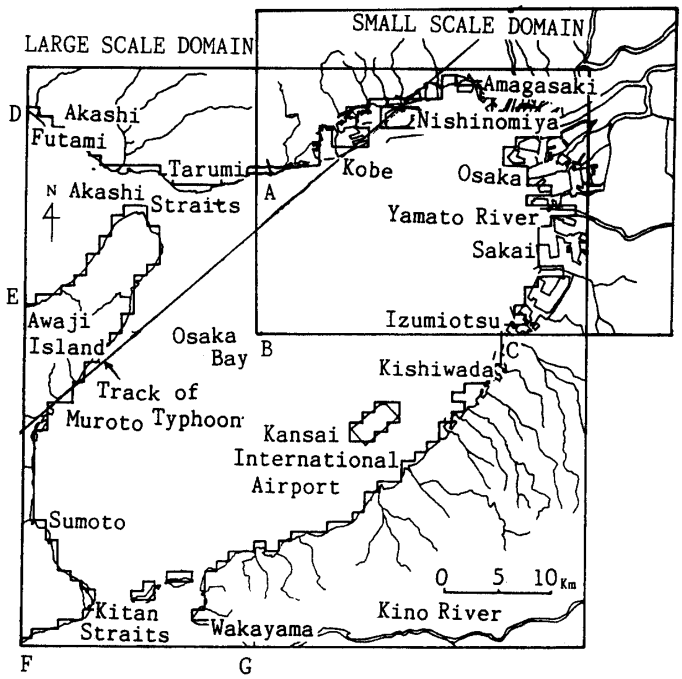

Fig. 6 Computational domains.

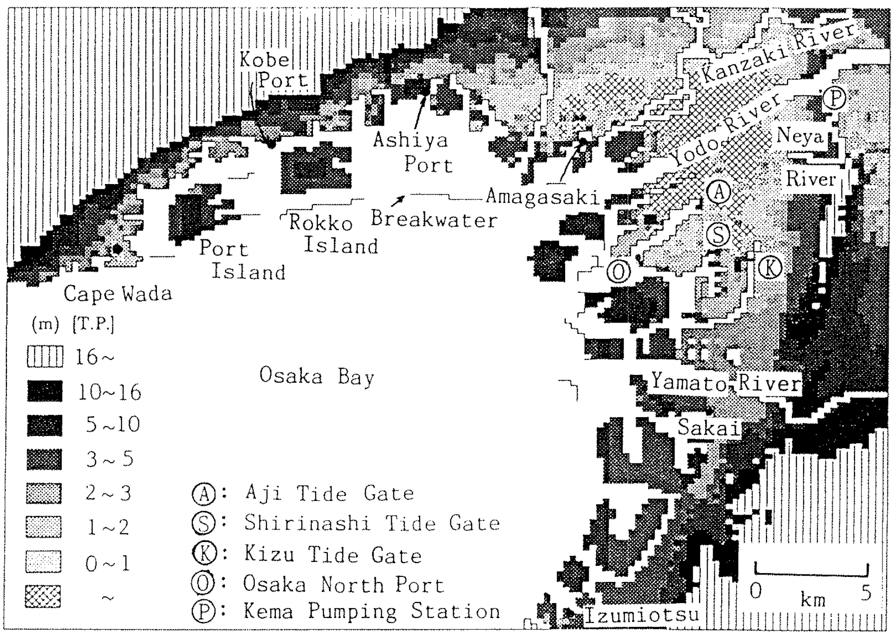

Fig. 7 Ground elevation in the small scale domain.

year plan to reconstruct high-tide embankments was implemented. At that time, various administrative measures were taken to regulate the pumping out of ground water in order to prevent further subsidence.

Since 1965, increased efforts have been made to cope with the most dangerous typhoon (hereafter called the "designed typhoon", the scale of which is the same as the Ise Bay Typhoon, and the course of which is the same as the Muroto Typhoon). The local government's Permanent Plan consists of three parts: construction of embankments, tide gates, and pumping stations. In 1970, three arch gates, the Aji, Shirinashi, and Kizu tide gates were constructed. Their locations are shown in **Fig. 7**. Moreover, high-

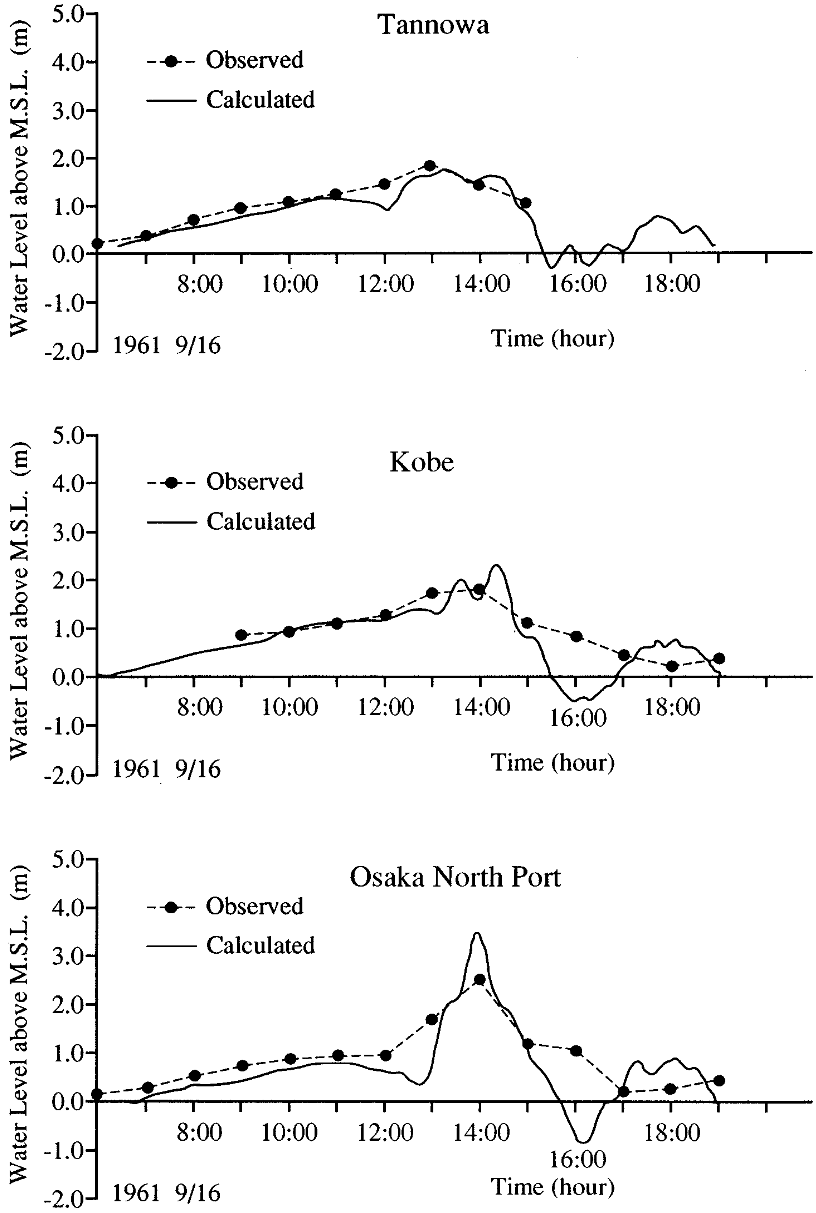

Fig. 8 Comparison of calculated and recorded water levels.

rise embankments were erected, completing the front line against high tides. In 1981, the Kema Pumping Station was established to discharge inland river water from the Neya River into the Yodo River when the tide gates are closed.

The heights of the embankments needed downstream of tide gate H_d and upstream of tide gate H_u in the Yodo River System were determined from the following expressions [9]:

Downstream of the Tide Gate

$$H_d = H_1 + H_2 + H_3$$

where H_1 is the mean high water level during the typhoon season (from July to November); O.P.+2.2 m; H_2=3.0 m, the estimated anomaly of the storm surge when a typhoon of a scale similar to that produced by the Ise Bay Typhoon hits Osaka Bay during the time of high water; and H_3 is a height of free-board of 1.4 m. The height of the embankment needed downstream of the tide gate therefore is O.P.+6.6 m. The height of each tide gate is O.P.+7.4 m.

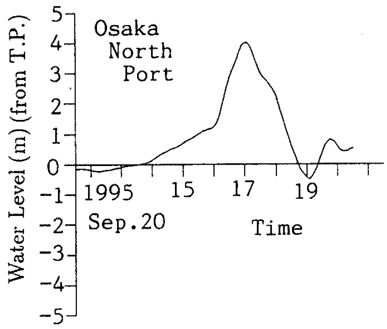

Fig. 9 Temporal change in the water level for the designed typhoon.

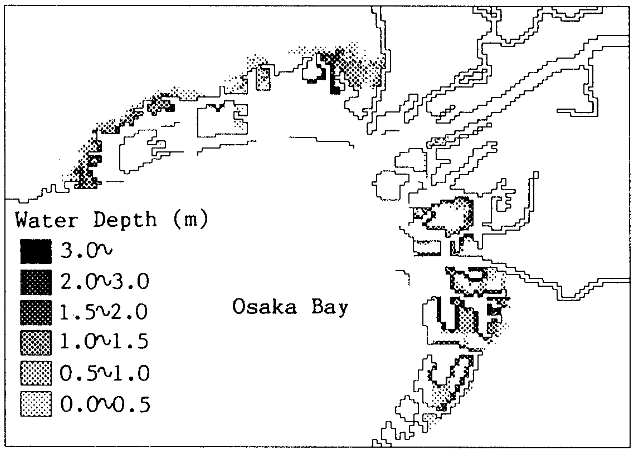

Fig. 10 Calculated areas flooded in the designed typhoon (maximum water depth).

Upstream of the Tide Gate

$$H_u = H_4 + H_5$$

where H_4 is the water level upstream of the tide gate, O.P.+3.5 m and H_5 the height of free-board, 0.8 m. The height of the embankment needed upstream of the tide gate therefore is O.P.+4.3 m.

In the Kanzaki River System, the countermeasures needed against the high water level caused by storm surges are embankments. Here the heights of the needed embankments are O.P.+8.1 m (=H_1+H_2+2.9 m [height of free-board]) at the river mouth and O.P.+6.0 m (=H_1+H_2+0.8 m [height of free-board]) elsewhere.

3.3 *Efficacy of the Current Countermeasures against Storm Surges*

To check the efficacy of the current countermeasures against storm surges in the cities of the Osaka Bay area, a numerical simulation of storm surge flooding was made. **Fig. 9** shows temporal changes in the water level at Osaka's North Port for the "designed typhoon" of September 20, 1995. The peak height is about 4.0 m from T.P. (=O.P.+5.3 m, and the relation between T.P. and O.P. is O.P.=T.P.+1.3 m). This is about 1 m greater than the value recorded in the Dai-ni Muroto Typhoon. **Fig. 10** shows the calculated maximum flooded water depth distribution for this "designed typhoon". The main part of Osaka City is not flooded; therefore, current countermeasures to prevent storm surge disasters within that city are considered to be effective, but some parts of the cities of Kobe, Ashiya, and Sakai are flooded.

4. VARIATION IN THE AREA FLOODED DUE TO VARIATION IN TYPHOON CHARACTERISTICS

4.1 *Relation between the Typhoon Course and Area Flooded*

Osaka City has taken measures against storm surges generated by a "designed typhoon", the course of which is the same as Muroto Typhoon; but, it is not clear whether this is the worst possible course for cities in the Osaka Bay area. By changing typhoon characteristics, we could establish the worst course for cities in the Osaka Bay area. **Fig. 11** shows 13 tracking paths which were moved between 60 km eastward and westward parallel to the Muroto Typhoon path at intervals of 10 km. These paths were investigated to establish the worst typhoon path for cities in the Osaka Bay area.

We defined as the "worst typhoon" one whose path generated maximum flooded areas in the small scale region, whose speed was the same as that of the Muroto Typhoon, whose central pressure was 920 hPa and maximum wind radius 60 km, and which attacked the bay areas during high tide. **Fig. 12** shows the relation between each typhoon path and temporal change in the flooded areas in the small scale region. When a typhoon takes the path 30 km west of and parallel to that of the Muroto Typhoon, it is the worst course for cities in the Osaka Bay area. We designated it the "worst typhoon". The reason the 30 km westward path is the worst one for this area is because the radius of the maximum typhonic wind speed, r_m, used was 60 km and the super-gradient wind effect was considered. The actual maximum wind speed occurred at $\xi_p=r/r_m=0.5$ i.e. $r=0.5\times60=30$ km. This means that the maximum wind speed was 30 km east of the center of the "worst typhoon". The worst path is not that of the center of a typhoon running through Osaka Bay longitudinally but that of the maximum wind field, a position 30 km east of the center of that typhoon (dashed line in **Fig. 11**). Of course, these results depend only on the typhoon model. They are not necessarily those for natural typhoon phenomena.

Fig. 13 shows the distribution of the maximum water depth produced by storm surges generated by the "worst typhoon". The scale of inundation is larger than that of the "designed typhoon" (see **Fig. 10**), and flooding more than 2 m deep occurs at Sakai, Nishinomiya, Ashiya, and Kobe, whereas a large part of Osaka City is not inundated. Consequently, it can be said that the "worst typhoon" path is a more

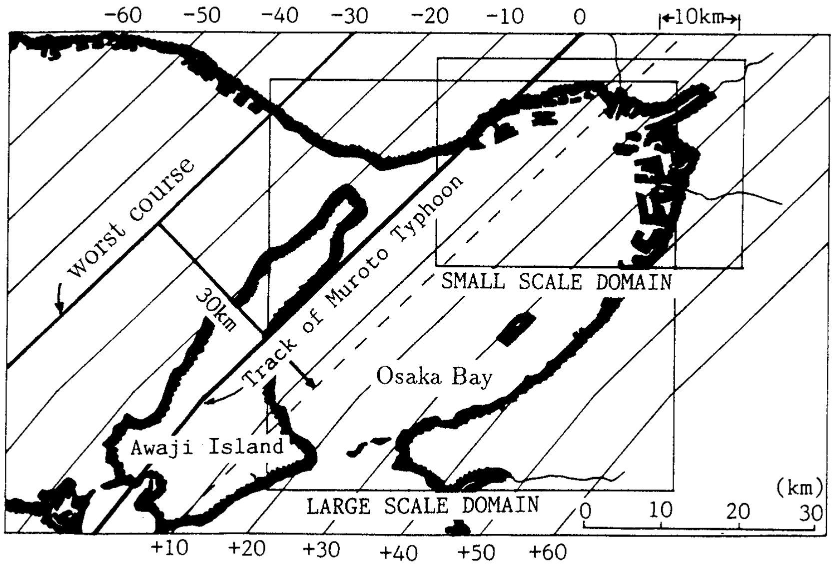

Fig. 11 Thirteen tracking paths parallel to the path of Muroto Typhoon studied to find the "worst typhoon" path.

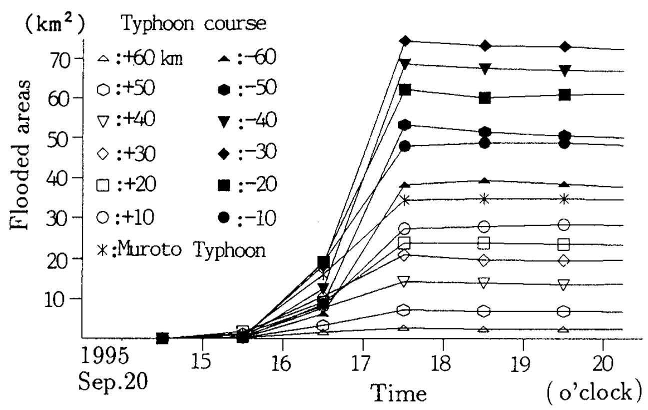

Fig. 12 Relation between each typhoon path and temporal change in areas flooded in the small scale region.

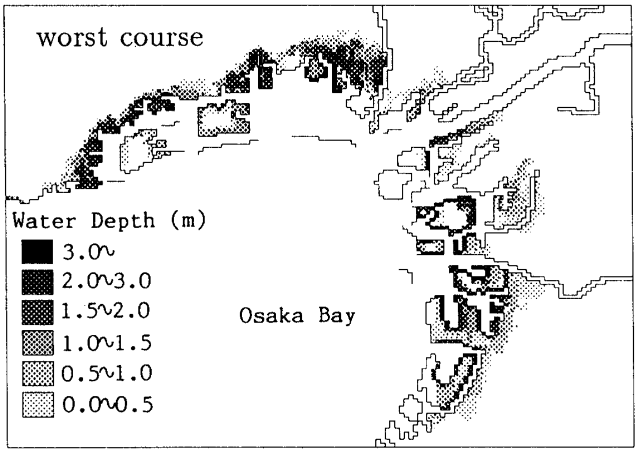

Fig. 13 Distribution of maximum water depth due to storm surges generated by the "worst typhoon".

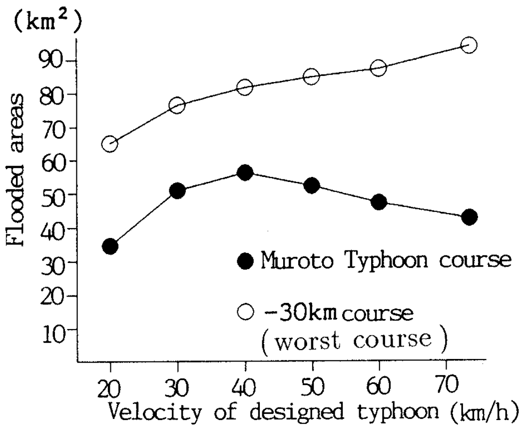

Fig. 14 Relation between the speeds of two typhoons and the calculated areas flooded.

dangerous one than that of the "designed typhoon".

4.2 *Relation between Typhoon Speed and the Area Flooded*

Fig. 14 shows the relation between typhoon speed and the calculated maximal areas flooded by storm surges. Note that in **Fig. 12** the areas flooded are the maximum areas flooded recorded at one-hour intervals. In **Fig. 14**, the open circles denote the results of the "worst typhoon" and closed circles those of the Muroto Typhoon. In the latter, the flooded areas take the maximum value of about 60 km^2 at the typhoon speed of 40 km/h, and even should the speed increase, the flooded areas decrease. This is because when the ratio of the typhoon speed, C, to the propagation speed of the long waves, $\sqrt{gh}$, takes a value of about 0.8 resonance occurs [10], and the storm surge height becomes large for the effect of the drop in pressure. In this case, the value of the ratio is estimated to be about 0.8 for h=20 m, g=9.8 m/s^2 and C=40 km/h (=11.11 m/s). In contrast, the faster the typhoon moves, the larger the areas flooded in the "worst typhoon". This is because the effects of the wind set-up are more significant than those of the drop in atmospheric pressure for the "worst typhoon".

5. VARIATION IN AREAS FLOODED DUE TO SEA LEVEL RISES

Increases of 3°C in temperature and 65 cm in sea level are predicted by the end of the 21st century because of global greenhouse effects [11]. Therefore there is danger of large-scale inundations due to storm surges and/or decreases in the discharge capacity at river mouths.

If in the future such phenomena occur at the sites of big cities such as Osaka, which have highly concentrated populations, as well as personal, business and public properties, and intricate life-line systems, very serious damage could occur. We therefore estimated the extent of inundation that would be caused by a "designed typhoon" on September 21, 2100, on the assumption that the mean sea level in Osaka Bay has increased 65 cm.

Fig. 15 shows temporal changes in the water level for the rise in sea level at Osaka's North Port. The peak water level is about 4.6 m from T.P. (=O.P.+5.9 m). This value is about 65 cm higher than that calculated for a "designed typhoon" before the rise in sea level. This increment corresponds to the rise in sea level produced by global greenhouse effects. **Fig. 16** shows the results calculated for the distribution of maximum water depth after this sea level rise. The flooded area is larger than that for the "designed typhoon" before the rise in sea level. The total flooded area now is about 63 km² whereas before the rise in sea level it was 35 km². A rise in sea level of 65 cm generates severe inundation, the area flooded being about 1.8 times that found for the "designed typhoon" prior to the rise in sea level. Note, however, that there are scarcely any flooded areas in Osaka City, itself. This means that the countermeasure of having tide gates with heights of O.P.+6.6 m is effective. As the effect of wave overtopping on inundation is not considered in this calculation, further discussion of this effect is needed. If the predicted value for the rise in sea level is valid, new countermeasures against storm surges after the rise in sea level will be necessary; e.g., in the cities of Kobe and Nishinomiya.

6. CONCLUSIONS

The method by which we estimated the occurrence of storm surges and the results of flooding in protected low-lying areas has been shown to be very useful for assessing countermeasures taken against storm surges: Actual temporal changes in the water level produced by the Dai-ni Muroto Typhoon are relatively well explained by this simulation method. The efficacy of the current countermeasures against storm surges in Osaka Bay could be evaluated from calculations made for a "designed typhoon". We

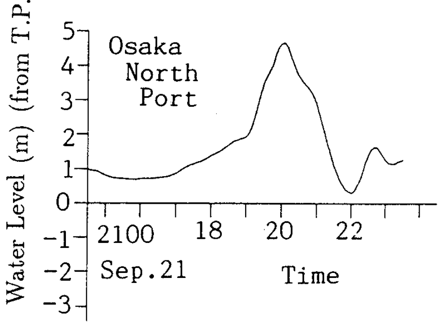

Fig. 15 Temporal change in the water level for a rise in sea level.

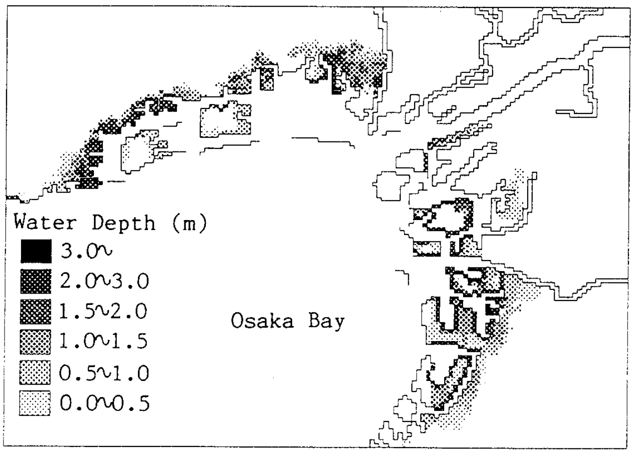

Fig. 16 The calculated areas flooded after a rise in sea level (maximum water depth).

found that the main parts of Osaka City would not be inundated by the storm surges produced because of protection by existing countermeasures. Extensive areas of the nearby cities of Kobe, Ashiya, and Sakai, however, would be flooded. Further countermeasures against storm surges therefore must be developed for these cities. The worst course for a typhoon in the Osaka Bay area was established on the basis of the areas flooded by storm surges. A typhoon taking a path 30 km west of and parallel to that of the Muroto Typhoon generates the most severe flooding in cities in the Osaka bay area. The influence of the speed of the typhoon on the area flooded also was investigated. Flooded areas had a maximum value of about 60 km^2 at a typhoon speed of 40 km/h; but, even if the speed increased, the areas flooded were fewer in the Muroto Typhoon. In contrast, the faster the typhoon moved, the larger the areas of flooding in the case of the "worst typhoon". The reason was that the effects of the wind set-up were more marked than those of the drop in atmospheric pressure for the "worst typhoon", whereas resonance was an important factor in the Muroto Typhoon.

Zones at risk of storm surge flooding after the 21st century rise in sea level caused by the greenhouse effects also could be predicted by this simulation model. A rise in sea level of 65 cm would cause severe inundation in an area about 1.8 times that flooded in the "designed typhoon" prior to the rise in sea level. If the predicted rise in sea level is valid, new countermeasures will have to be taken against storm surges in the Osaka Bay area. Our simulation model and the results calculated from it provide the basis for the design of new countermeasures.

ACKNOWLEDGMENTS

Parts of this study were supported by Grants-in-Aid for General Scientific Research (B) [No. 05452376] and (C) [05680368] from the Japanese Ministry of Education, Sciece, Sports and Culture. We express our gratitude to the authorities concerned.

REFERENCES

[1] Iwagaki, Y. and Sawaragi, T. (1982)., Coastal Engineering, *Kyoritsu Shuppan*, p.224 (in Japanese).

[2] Committee of Hydraulics, JSCE (1985)., Handbook of hydraulic engineering, *Gihodo*, pp.287-288 (in Japanese).

[3] Fujii, T. and Mitsuta, Y. (1986)., Synthesis of a stochastic typhoon model and simulation of typhoon wind, *Annuals, Disas. Prev. Res. Inst., Kyoto Univ.*, No.29B-1, pp.229-239 (in Japanese).

[4] Katsura, J. et al. (1992)., Storm surge and severe wind disasters caused by the 1991 cyclone in Bangladesh, *Research Report on Natural Disasters*, Supported by the Japanese Ministry of Education, Science and Culture (Grant No.03306020), Japanese Group for the Study of Natural Disaster Science, pp.54-82.

[5] Mitsuta, Y., Monji, N., Tsukamoto, O. and Asai, H. (1978)., Meteorological study of Typhoon 7705, *Annuals, Disas. Prev. Res. Inst., Kyoto Univ.*, No.21B-1, pp.405-415 (in Japanese).

[6] Yamamoto, R., Mitsuta, Y., Monji, N., Tsukamoto, O. and Suenobu, T.(1978)., Meteorological study of Typhoon 7709, *Annuals, Disas. Prev. Res. Inst., Kyoto Univ.*, No.21B-1, pp.417-425 (in Japanese).

[7] Nakagawa, H. (1992)., Behavior of overland flood flow or debris flow and its analysis, *Lecture Note for Water Eng.*, Committee of Hydraulics, JSCE, pp.A-9-1-A-9-20 (in Japanese).

[8] Nakatsuji, K., Watanabe, S., Kurita, H. and Yamane, N. (1993)., Greenhouse effects on storm surges: A Case study at Osaka Bay, Japan, *Proc. XXV Cong. of IAHR*, Vol.IV, pp.56-63.

[9] Osaka Prefectural Government., Comprehensive flood control measures in urban area, *Pamphlet published by the Urban River Division, Departments of Public Works*, pp.2-5.

[10] Tsuchiya, Y. et al. (1980)., Characteristics of storm surges due to Typhoon 7916, Report on the "Comprehensive research on strong wind and flood disaster due to Typhoon 7916", organized by Murota, A, *Research Report on Natural Disasters*, Supported by the Japanese Ministry of Education, Science and Culture (No. B-54-1), 69p. (in Japanese).

[11] Kasumigaseki Society for Research on Global Warming (1991)., Summary of the report of the intergovernmental panel on climate change, *Chuo Houki*, pp.75-78 (in Japanese).